arXiv:hep-ph/9601393v1 1 Feb 1996

UCD-96-04
January 1996

# HIGGS BOSON AND $W_L W_L$ SCATTERING AT $e^- e^-$ COLLIDERS *

TAO HAN
*Davis Institute for High Energy Physics*
*Department of Physics, University of California, Davis, CA 95616, USA*

**Abstract**

We discuss the Standard-Model Higgs boson production in the channels $e^-e^- \to e^-e^-H$, $e^-\nu W^-H$, and $e^-e^-ZH$. We also illustrate the enhancements in the $W^-W^-$ cross section that would result from a strongly-interacting Higgs sector or from a $H^{--}$ resonance in a doublet + triplet scalar field model.

## 1 Introduction

High-energy experiments at $e^+e^-$ colliders have proved to be very fruitful. The construction of high energy $e^-e^-$ colliders has not been pursued as actively. The probable reason for this lack of activity is the absence of $s$-channel resonance production and pair production for new particles in $e^-e^-$ collisions due to lepton number conservation. However, precisely because direct channel resonances are not expected, high energy $e^-e^-$ collisions could be a clean way to uncover physics beyond the Standard Model (SM). This has become evident from the works presented in this workshop.[1]

In this presentation, we discuss the production of the standard model (SM) Higgs boson ($H$), and the associated production with a weak boson. We also study the possibility of detecting strong $W^-W^-$ scattering in the

*Contribution to the Proceedings of $e^-e^-$ Workshop, Santa Cruz, CA, Sept. 4–5, 1995.

$I = 2$ channel, which is unique for an $e^-e^-$ collider, and quantitatively evaluate the enhancement of $W^-W^-$ production due to a doubly-charged Higgs boson. The results presented here are essentially based on two recent papers.[2, 3]

# 2 SM Higgs Boson Production

In $e^-e^-$ collisions single Higgs boson production at lowest order can occur via the processes

$$e^-e^- \to e^-e^-H\ ,\quad e^-e^- \to e^-\nu_e W^-H\ ,\quad e^-e^- \to e^-e^-ZH. \tag{1}$$

The cross sections are shown in Fig. 1(a) versus c. m. energy $\sqrt{s}$ for

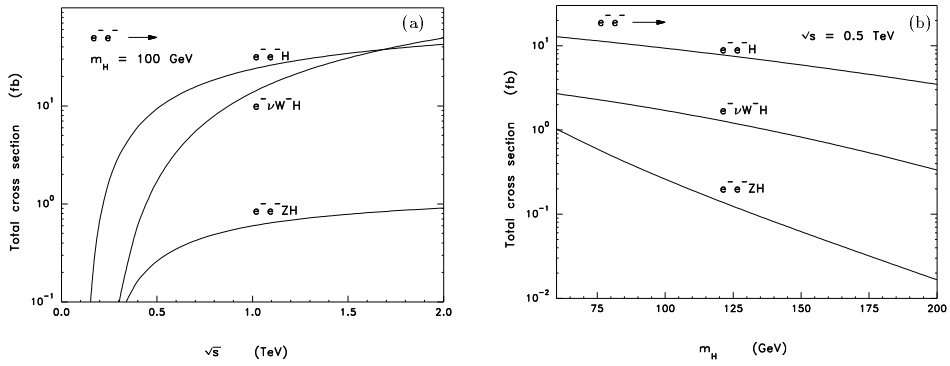



Figure 1: Cross sections for production of the Standard-Model Higgs boson in $e^-e^-$ collisions (a) versus $\sqrt{s}$ at $m_H = 100$ GeV, (b) versus $m_H$ at $\sqrt{s} = 0.5$ TeV.

$m_H = 100$ GeV and (b) versus $m_H$ at $\sqrt{s} = 0.5$ TeV. For $m_H = 100$ GeV and $\sqrt{s} = 0.5$ TeV the cross section is 9 fb for $e^-e^- \to e^-e^-H$ via $Z^*Z^* \to H$. In comparison, the Higgs production cross sections in $e^+e^-$ collisions for the same $\sqrt{s}$ and $m_H$ are 95 fb for $W^{+*}W^{-*} \to H$ and 60 fb for $Z^* \to ZH$ mechanisms.[4] Searching for the SM Higgs boson in $e^-e^-$ collisions is limited by the rather small cross sections, especially for heavier $m_H$.

For $m_H < 150$ GeV or so, the Higgs boson decays dominantly to $b\bar{b}$ and a Higgs signal identification is quite feasible. The only complication comes from the case in which $m_H$ is close to $M_Z$, when the $Z$-production processes

$$e^-e^- \to e^-e^-Z\ ,\ \ e^-e^- \to e^-\nu_e W^-Z\ ,\ \ e^-e^- \to e^-e^-ZZ \tag{2}$$

are large backgrounds to the Higgs processes (1) respectively. For example, for the production of a 100 GeV Higgs boson at $\sqrt{s} = 0.5$ TeV, $\sigma(e^-e^- \to e^-e^-H \to e^-e^-b\bar{b}) \approx 9$ fb and $\sigma(e^-e^- \to e^-e^-Z \to e^-e^-b\bar{b}) \approx 1100$ fb (with $B(Z \to b\bar{b}) = 15.5\%$). However, it is important to notice that the Higgs signal is very distinctive. The $H$-production is central while the $Z$-production is peaked at forward and backward scattering angles; thus the $Z$ background can be selectively suppressed by angular cuts.

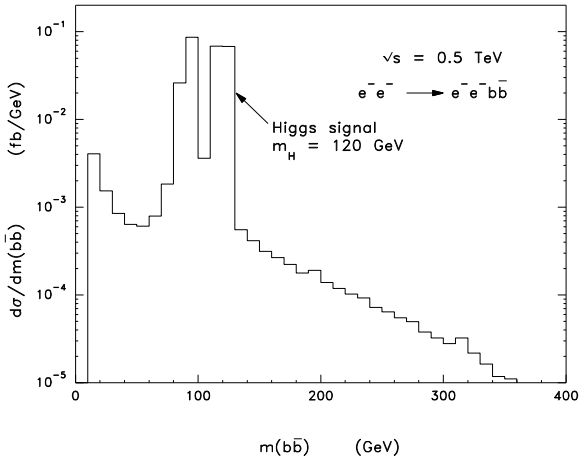



Figure 2: The differential cross section $d\sigma/dm(b\bar{b})$ versus the invariant mass $m(b\bar{b})$ of the $b\bar{b}$ pair in the process with the acceptance cuts of Eqs. (3) and (4). The peak at $m(b\bar{b}) \approx M_Z$ is due to $e^-e^- \to e^-e^-Z$ with $Z \to b\bar{b}$. The signal due to a Higgs boson of mass $m_H = 120$ GeV is illustrated.

To address the $H$ signal observability quantitatively, we evaluate the complete $e^-e^- \to e^-e^-b\bar{b}$ background including both $e^-e^- \to e^-e^-Z$ with $Z \to b\bar{b}$ and the two-photon production of $b\bar{b}$. Based on the fact that the two-photon background can be reduced substantially by keeping the photon

Table 1: The Higgs boson signal in the production of $e^-e^- \to e^-e^-H$ for $m_H = 60$–$140$ GeV and the background from $e^-e^- \to e^-e^-b\bar{b}$ with the invariant mass of the $b\bar{b}$ pair in the range $m_H \pm \Delta m_H$, with $\Delta m_H = 10$ GeV. For simplicity we take $\mathrm{B}(H \to b\bar{b}) = 1$, and assume that all the signal falls within $m_H \pm \Delta m_H$. The acceptance cuts are $p_{Te} > 15$ GeV and $|\cos\theta_e| < \cos(15^\circ)$ on the final state electrons, and $p_{Tb} > 25$ GeV and $|\cos\theta_b| < 0.7$ on the final state $b$'s.

| $m_H$ | Signal (fb) | Background (fb) |
|---|---|---|
| 60 | 1.4 | 0.02 |
| 70 | 1.4 | 0.03 |
| 80 | 1.4 | 0.27 |
| 90 | 1.4 | 1.1 |
| 100 | 1.4 | 0.86 |
| 120 | 1.3 | 0.02 |
| 140 | 1.3 | 0.01 |

propagators far off-shell, we impose the following acceptance cuts

$$p_{Te} > 15 \text{ GeV} \qquad \text{and} \qquad |\cos\theta_e| < \cos(15^\circ) \,, \tag{3}$$

on both of the electrons in the final state. We also impose the following acceptance cuts on the $b$'s in the final state (since the $b$'s in the signal events are populated at high transverse momenta $\approx m_H/2$):

$$p_{Tb} > 25 \text{ GeV} \qquad \text{and} \qquad |\cos\theta_b| < 0.7 \,. \tag{4}$$

After imposing (3) and (4), the Higgs signal is 1.4 fb for $m_H = 100$ GeV while the total $eeb\bar{b}$ background integrated over all $m(b\bar{b})$ is 1.3 fb. The background has a wide $m(b\bar{b})$ invariant mass distribution (see Fig. 2) with a peak at $m(b\bar{b}) = M_Z$ due to $e^-e^- \to e^-e^-Z$. The signal is a sharp peak at the Higgs mass. We consider an invariant mass resolution $\Delta m_H$ for the $b\bar{b}$ pair of 10 GeV and assume that all the signal falls within $m_H \pm \Delta m_H$. The signal and the background in such bins at various Higgs mass values are summarized in Table 1. In this simple comparison we have assumed perfect $b$-tagging with only the $b\bar{b}$ final state counted as background, *i.e.*, the other $q\bar{q}$ ($q = u, d, s, c$) final states are rejected. The background for $m_H = 90$ GeV

is the largest because of $ee \to eeZ$. We conclude that the intermediate mass Higgs boson in the channel $e^-e^- \to e^-e^-H$ with $H \to b\bar{b}$ may be observable with an integrated luminosity of 20 fb$^{-1}$.

When $m_H > 2m_Z$, Higgs production with $H \to ZZ$ decay can give an appreciable enhancement to the $e^-e^- \to e^-e^-ZZ$ production; for example, at $m_H = 200$ GeV the cross section of $e^-e^- \to e^-e^-ZZ$ is a factor of two larger than that with $m_H = 100$ GeV.

# 3 Strong $W_L^-W_L^-$ Scattering Signal

If no light Higgs boson is found for $m_H$ to be less than about 800 GeV, one would anticipate that the interactions among longitudinal vector bosons become strong.[5] An $e^-e^-$ collider offers a unique opportunity to explore the weak isospin $I = 2$ $s$-channel[6] via the process $W_L^-W_L^- \to W_L^-W_L^-$.[7] The simplest model for a strongly-interacting $W_L^-W_L^-$ sector is the exchange of a heavy Higgs boson. This results in an enhancement of the $e^-e^- \to \nu\nu W^-W^-$ production cross section compared to that expected from the exchange of a light Higgs boson. This enhancement due to a Higgs boson of mass 1 TeV can be defined as the difference of the $W_L^-W_L^- \to W_L^-W_L^-$ fusion contributions

$$\Delta\sigma_H = \sigma(m_H = 1 \text{ TeV}) - \sigma(m_H = 0.1 \text{ TeV}) \tag{5}$$

to $e^-e^- \to \nu\nu W^-W^-$ production. There is no appreciable numerical change between the choices $m_H = 0.1$ TeV and $m_H = 0$ for the light Higgs boson reference mass. We find the values

$$\Delta\sigma_H \simeq \begin{cases} 53.6 - 50.9 = 2.7 \text{ fb} & \text{at } \sqrt{s} = 1.5 \text{ TeV}; \\ 86.5 - 82.0 = 4.5 \text{ fb} & \text{at } \sqrt{s} = 2 \text{ TeV}. \end{cases} \tag{6}$$

We first address the observability of this strong $W_L^-W_L^- \to W_L^-W_L^-$ signal at $\sqrt{s} = 2$ TeV. The cross section for $e^-e^- \to \nu\nu W^-W^-$ from all Standard-Model diagrams (dominantly $W_T^-W_T^-$) is about 20 times larger than $\Delta\sigma$. Hence the background contributions associated with transverse $W$ bosons ($W_T^-W_T^-$, $W_T^-W_L^-$) must somehow be selectively reduced by acceptance criteria if we are to observe the strongly-interacting $W_L^-W_L^-$ signal.

There are several ways to accomplish the substantial background suppression.[6, 7, 8] The $W_L^-W_L^-$ scattering process gives large $M(W^-W^-)$ of order 1 TeV

with centrally-produced $W^-$ having large $p_T$. Thus we impose the kinematic cuts

$$p_T(W) > 150 \text{ GeV}, \quad |\cos\theta_W| < 0.8\,, \tag{7}$$

which retains about one-third of the signal and reduces the SM backgrounds by more than an order of magnitude. After those cuts, the heavy Higgs enhancement becomes $\Delta\sigma_H \simeq 7.8 - 6.3 = 1.5$ fb.

In hadronic $W$-decays, the sign of the $W$ charge is not identified and the two-photon process $e^-e^- \to e^-e^-W^+W^-$ may also present a substantial background when the final electrons are not observed. The cross section for $e^-e^- \to e^-e^-W^+W^-$ is about a factor of 30 larger than $e^-e^- \to \nu\nu W^-W^-$. Moreover, $e^-e^- \to e^-\nu W^-Z$ could add to the background if the reconstructed invariant masses in hadronic decays are not sufficiently resolved to distinguish $W$ from $Z$. In order to suppress these backgrounds we veto events in which an electron can be identified having

$$E_e > 50 \text{ GeV}, \quad |\cos\theta_e| < |\cos(150 \text{ mrad})|\,. \tag{8}$$

With the acceptance of Eqs. (7) and (8), the remaining $e^-e^- \to e^-e^-W^+W^-$ and $e^-e^- \to e^-\nu_e W^-Z$ backgrounds are 60 fb and 10 fb, respectively.

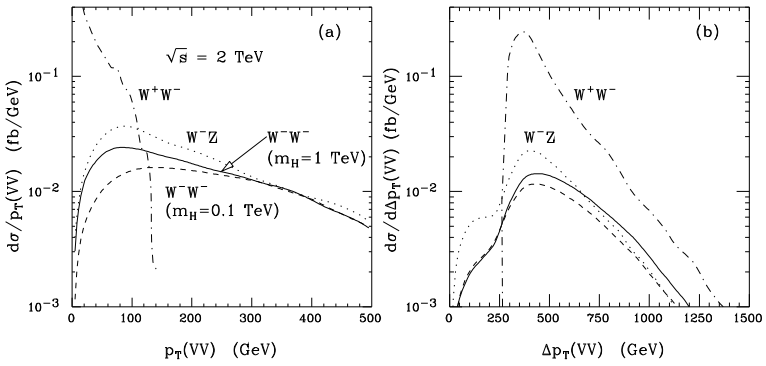



Figure 3: Distributions at $\sqrt{s} = 2$ TeV in the transverse momenta of vector bosons produced in the reactions $e^-e^- \to \nu\nu W^-W^-, e^-e^-W^+W^-, e^-\nu W^-Z$: (a) $p_T(VV) = |\mathbf{p}_T(V_1) + \mathbf{p}_T(V_2)|$, (b) $\Delta p_T(VV) = |\mathbf{p}_T(V_1) - \mathbf{p}_T(V_2)|$.

A further improvement in isolating the $W_L^- W_L^-$ signal derives from the fact that the $p_T(WW)$ spectrum of the signal is peaked around $M_W$ and falls off rapidly at high $p_T$ like $1/p_T^4$. Figure 3(a) compares the $p_T(VV)$ distribution of the $W_L^- W_L^-$ signal with the backgrounds. Note that the difference between the solid curve (with $m_H = 1$ TeV) and the dashed curve (with $m_H = 0.1$ TeV) is the strong $W_L^- W_L^-$ enhancement. We impose the selection

$$50 \text{ GeV} < p_T(VV) < 300 \text{ GeV} \tag{9}$$

for additional background suppression.

The signal gives $W_L^-$ bosons that are fast and moving back-to-back in the transverse plane. The difference in the transverse momenta of the two weak bosons is

$$\Delta p_T(VV) = |\mathbf{p}_T(V_1) - \mathbf{p}_T(V_2)| \tag{10}$$

presented in Fig. 3(b). The signal (difference of solid and dashed curves) is enhanced by the cut

$$\Delta p_T(VV) > 400 \text{ GeV}\,. \tag{11}$$

With the additional cuts of Eqs. (9) and (11) the surviving signal is

$$\Delta\sigma_H \simeq 3.8 - 2.8 = 1.0 \text{ fb}\,. \tag{12}$$

The efficiency for retaining the signal with such cuts is 67%. The remaining backgrounds are 4.4 fb for $e^-e^- \to e^-e^-W^-W^+$ and 4.7 fb for $e^-e^- \to e^-\nu W^- Z$. The resulting $M(VV)$ distributions after these cuts are presented in Fig. 4. At high $VV$ invariant masses the strong $W_L^- W_L^-$ scattering rate due to the exchange of a 1 TeV Higgs boson is enhanced over the $W_T^- W_T^-$, $W_T^- W_L^-$ and $W^-W^+$ backgrounds, while the background due to $W^-Z$ still persists.

Next we estimate the signal rates for other strongly-interacting scenarios. We consider a chirally-coupled scalar boson ($m_S = 1$ TeV and $\Gamma_S = 350$ GeV), a chirally-coupled vector boson ($m_V = 1$ TeV and $\Gamma_V = 25$ GeV),[7, 8] and the low energy theorem amplitude.[8] These calculations are carried out with the effective $W$-boson approximation (EWA). In this calculational method one is unable to obtain the exact kinematics for the final state of $W^-W^-$. In order to simulate the acceptance effects of Eqs. (9) and (11), we multiplied the EWA calculations by the efficiency factor 67% found in the heavy Higgs boson model.

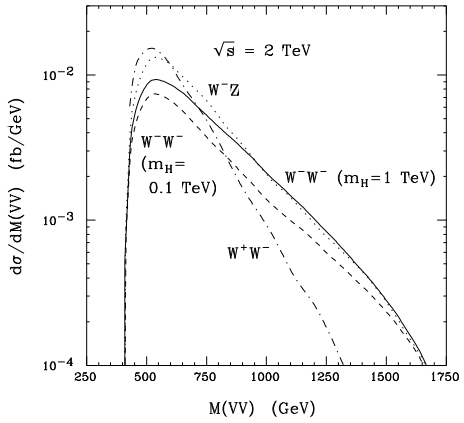



Figure 4: Invariant mass distributions of the weak boson pairs produced in the reactions $e^-e^- \to \nu\nu W^-W^-, e^-e^-W^+W^-, e^-\nu W^-Z$ after the acceptance cuts of Eqs. (9) and (11) have been applied to enhance the strongly-interacting $W^-W^-$ signal due to the exchange of a 1 TeV SM Higgs boson.

The predicted cross sections at $\sqrt{s} = 2$ TeV with the cuts discussed above are presented in Table 2. The number of events with hadronic $W, Z$ decays are given for an integrated luminosity of 300 fb$^{-1}$. In Table 2 we see that the backgrounds (dominantly from $W^-Z$ production) to the signals are still substantial after the kinematic selection criteria. Due to the absence of an $s$-channel resonance, the signals are mostly an overall enhancement on the $M_{WW}$ spectrum. If we can predict the SM backgrounds at a level of better than 10%, there is a chance that we can observe the strong $W^-W^-$ scattering via the hadronic decay modes at statistical significance $S/\sqrt{B} > 4$ for a 1 TeV scalar or a vector particle, and at $S/\sqrt{B} \geq 6.4$ for the LET amplitude with $M_{WW} > 500$ GeV.

At $\sqrt{s} = 1.5$ TeV, the signal rate is reduced by 40%, as shown in Eq. (6), which makes the signal observation more difficult. An improvement was made to include the $W/Z$ discrimination through the di-jet mass of their decay products. Typically, one assumes the jet energy resolution to be[9]

$$\delta E_j/E_j = 0.50\Big/\sqrt{E_j} \ \oplus \ 0.02 \ , \tag{13}$$

in GeV units (where the symbol $\oplus$ means adding in quadrature). If we now

Table 2: Signals at $\sqrt{s} = 2$ TeV from different models of strongly-interacting $W^-W^-$ with cuts discussed in the text. Backgrounds are summed over $W^-W^-$ with a light Higgs exchange, $W^+W^-$, and $W^-Z$. Entries correspond to the number of events with hadronic $W, Z$ decays for an integrated luminosity of 300 fb$^{-1}$ and those in parentheses are in units of fb without the branching fractions. As a rough indication of the signal observability, values of $S/\sqrt{B}$ are also given.

| $\sqrt{s} = 2$ TeV<br>$M_{WW}^{min}$ | SM<br>$m_H = 1$ TeV | Scalar<br>$m_S = 1$ TeV | Vector<br>$m_V = 1$ TeV | LET | Bckgnds |
|---|---|---|---|---|---|
| 0.5 TeV | 130 (0.88) | 175 (1.2) | 167 (1.1) | 245 (1.7) | 1470 (10) |
| $S/\sqrt{B}$ | 3.4 | 4.6 | 4.4 | 6.4 | |
| 0.75 TeV | 65 (0.44) | 106 (0.72) | 93 (0.63) | 150 (1.0) | 515 (3.5) |
| $S/\sqrt{B}$ | 2.9 | 4.7 | 4.1 | 6.6 | |

identify dijets having measured mass in the intervals

$$\left[0.85M_W,\ \frac{1}{2}(M_W + M_Z)\right] \quad \text{and} \quad \left[\frac{1}{2}(M_W + M_Z),\ 1.15M_Z\right]$$

as $W \to jj$ and $Z \to jj$, respectively, then simulation[3] indicates that true $WW$, $WZ$, $ZZ \to jjjj$ events will be interpreted statistically as follows:

$$\begin{aligned}
WW &\Rightarrow 73\%\, WW,\ 17\%\, WZ,\ 1\%\, ZZ,\ 9\%\,\text{reject},\\
WZ &\Rightarrow 19\%\, WW,\ 66\%\, WZ,\ 7\%\, ZZ,\ 8\%\,\text{reject},\\
ZZ &\Rightarrow 5\%\, WW,\ 32\%\, WZ,\ 55\%\, ZZ,\ 8\%\,\text{reject}.
\end{aligned}$$

This helps improve the signal observability and the results are shown in Table 3.

The use of $Z \to e^+e^-, \mu^+\mu^-, b\bar{b}$ (with $b$-tagging), with combined branching fraction of about 22%, could be helpful in determining the contribution of the $W^-Z$ background process and further improving the signal identification.

# 4 $H^{--} \to W^-W^-$ Signal in Scalar Doublet + Triplet Model

A search for a doubly-charged Higgs boson in a model with a scalar triplet could also be carried out at an $e^-e^-$ collider. What makes the $e^-e^-$ col-

Table 3: Signals at $\sqrt{s} = 1.5$ TeV from different models of strongly-interacting $W^-W^-$ with cuts discussed in the text. Backgrounds are summed over $W^-W^-$ with a light Higgs exchange, $W^+W^-$, and $W^-Z$. Entries correspond to the number of events with hadronic $W, Z$ decays for an integrated luminosity of 300 fb$^{-1}$. $W/Z$ identification via dijet mass has been implemented, as discussed in the text to improve the signal/background ratio. As a rough indication of the signal observability, values of $S/\sqrt{B}$ are also given.

| $\sqrt{s} = 1.5$ TeV $M_{WW}^{min}$ | SM $m_H = 1$ TeV | Scalar $m_S = 1$ TeV | Vector $m_V = 1$ TeV | LET | Bckgnds |
|---|---|---|---|---|---|
| 0.5 TeV | 41 | 53 | 54 | 63 | 345 |
| $S/\sqrt{B}$ | 2.2 | 2.8 | 2.9 | 3.4 | |

lider unique in this instance is that the doubly-charged Higgs boson can be produced as an $s$-channel resonance. Jack Gunion[10] recently discussed the lepton-number violating process

$$e^-e^- \to H^{--}$$

and found interesting results. We here consider the process

$$W^-W^- \to H^{--}$$

followed by $H^{--} \to W^-W^-$ decays. Detailed analyses of the doublet plus triplet model can be found in the literature[11] and we will not repeat the discussion of the model here. With certain assumptions for simplicity, there are then two independent parameters left in the model:[2, 11] the mass parameter $M(H^{--})$ and the mixing angle $\theta_H$ between the Higgs doublet and the triplet fields, which is related to the ratio of the vacuum expectation values. Figure 5 presents the $M_{W^-W^-}$ distribution at $\sqrt{s} = 0.5$ TeV including the resonance process $e^-e^- \to \nu\nu H^{--} \to \nu\nu W^-W^-$ with $M(H^{--}) = 0.2$ or 0.3 GeV, taking maximum mixing $\tan\theta_H = 1$. A significant enhancement above the SM background occurs. If existed at all, such a doubly-charged Higgs boson should manifest itself in $e^-e^-$ collisions.

Discussions here should be essentially applicable for the doubly-charged vector bosons as well.[12]

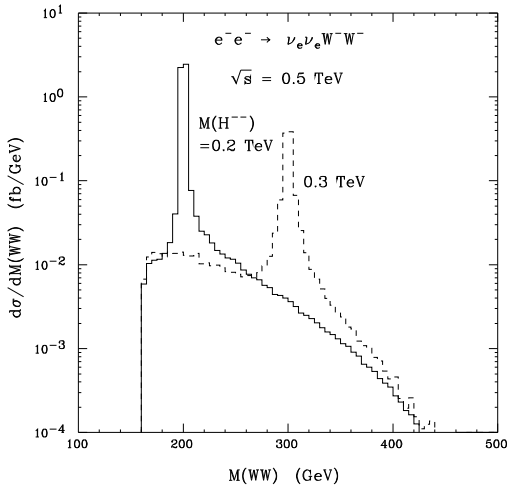



Figure 5: The distribution in the $W^-W^-$ invariant mass for $e^-e^- \to \nu_e\nu_e W^-W^-$ including the contribution of a doubly-charged Higgs boson of mass $M(H^{--}) = 0.2$ or 0.3 TeV.

# 5 Summary

We have calculated the single and associated Higgs boson production and found that they may give observable signals, although the cross sections are generally not as large as those in $e^+e^-$ collisions. We have also investigated the possibility of observing strong $W_L^-W_L^-$ scattering, which occurs through the weak isospin $I = 2$ channel and is unique to $e^-e^-$ collisions. We have developed certain kinematic cuts to significantly reduce the $W_T^-W_T^-$, $W_T^-W_L^-$, $W^+W^-$ and $W^-Z$ backgrounds to the strong $W_L^-W_L^-$ signal in hadronic decay modes. The $W^-Z$ background persists at large $M_{WW}$, which makes the observation of strong $W_L^-W_L^-$ scattering difficult. On the other hand, if good jet energy resolution can be obtained, then $W$ and $Z$ may be distinguished so that the "faked" background from $WZ$ final state may be further suppressed. If doubly-charged Higgs bosons exist, the $s$-channel enhancement in $W^-W^-$ final state would be very substantial at an $e^-e^-$ collider. Finally, by colliding $e_L^-$ beams the strong $W_L^-W_L^-$ signal in the process $e^-e^- \to \nu_e\nu_e W_L^-W_L^-$ can be enhanced over the $W^+W^-$, $ZZ$, and $W^-Z$ backgrounds. Similarly, the $H^{--}$ signal will be favored with the use of $e_L^-$ beams. This survey of cross

sections and processes should provide useful benchmarks for serious studies of the potential of such a machine for new physics discovery.

**Acknowledgments**

I thank V. Barger, J. Beacom, K. Cheung and R. Phillips for the collaboration that led to most of the results presented here. This work is supported in part by the U.S. Department of Energy under contract DE-FG03-91ER40674, and by the Davis Institute for High Energy Physics.

**References**

# References

[1] See contributions to these proceedings; C. Heusch, in *Proceedings of the Workshop on Physics and Experiments with Linear $e^+e^-$ Colliders*, Waikoloa, Hawaii (April 1993), ed. F. Harris *et al.* (World Scientific, 1993), pp. 895, 917.

[2] V. Barger, J. Beacom, K. Cheung and T. Han, Phys. Rev. **D50**, 6704 (1994).

[3] V. Barger, K. Cheung, T. Han and R. Phillips, Phys. Rev. **D52**, 3815 (1995).

[4] See *e. g.*, V. Barger, K. Cheung, B.A. Kniehl, and R.N.J. Phillips, Phys. Rev. **D46**, 3725 (1992).

[5] M.S. Chanowitz and M.K. Gaillard, Nucl. Phys. **B261**, 379 (1985).

[6] M. S. Chanowitz and M. Golden, Phys. Rev. Lett. **61**, 1053 (1988); **63**, 466(E) (1989); V. Barger, K. Cheung, T. Han, and R.J.N. Phillips, Phys. Rev. **D42**, 3052 (1990); D. Dicus, J.F. Gunion, and R. Vega, Phys. Lett. **258B**, 475 (1991); M. S. Berger and M. S. Chanowitz, Phys. Lett. **263B**, 509 (1991); M.S. Chanowitz and W. Kilgore, Phys. Lett. **B322**, 147 (1994).

[7] T. Han, in *Proceedings of the Workshop on Physics and Experiments with Linear $e^+e^-$ Colliders*, Waikoloa, Hawaii (April 1993), ed. F. Harris *et al.* (World Scientific, 1993), p. 270.

[8] J. Bagger, V. Barger, K. Cheung, J. Gunion, T. Han, G. Ladinsky, R. Rosenfeld and C.P. Yuan, Phys. Rev. **D49**, 1246 (1994); Phys. Rev. **D52**, 3878 (1995).

[9] A. Miyamoto, in proceedings of *JLC Workshop*, Tsukuba, 1990.

[10] J.F. Gunion, in these proceedings (hep-ph/9510350).

[11] J.F. Gunion, R. Vega, and J. Wudka, Phys. Rev. **D42**, 1673 (1990).

[12] P. Frampton, Phys. Rev. Lett. **69**, 2889 (1992); F. Pisano and V. Pleitez, Phys. Rev. **D46**, 410 (1992).